Chapter 3
Development of a Controlled in Situ Process for the Formation of Porous Anodic Alumina and Al Nanomesh From Thin Aluminum Films

T. Lebyedyeva, M. Skoryk, and P. Shpylovyy

3.1 Introduction

The researches on the formation of porous anodic alumina (PAA) films for use of their nanoscale properties can be divided into two main areas: growing oxide on a bulk aluminum and foils and on films deposited onto the substrate. The development of technological processes of PAA creation on bulk aluminum usually presumes the improvement of methods of ordered structures creation with implementation of a two-stage process of anodizing. This is where significant success has already been achieved [1]. However, the method of growing of ordered PAA on deposited thin aluminum films is yet to be discovered. Only the processes of nanopore ordering for PAA on thin Al films by pre-texturing by special stamps can be considered as those that secured proved results [2]. The structural difference in PAA films, grown on the bulk aluminum (plates or folds) and on the deposited films of aluminum, is usually attributed to the fact that on contrary to the annealed and subjected to the electrochemical polishing surface of bulk aluminum, the surface of the deposited film has high surface roughness, and films themselves may be disordered small-grain structure with a considerable difference in grain sizes and a large number of randomly distributed inter-grain boundaries. Aluminum films produced under various conditions also differ from each other—according to structural parameters, density of grains packing, and average values of surface roughness [3–5].

Nevertheless there are a lot of publications devoted to the nanostructures on substrates of various materials, including semiconductors, metals, dielectrics, and

T. Lebyedyeva (✉) · P. Shpylovyy
V.M. Glushkov Institute of Cybernetics, National Academy of Sciences of Ukraine, Kyiv, Ukraine

M. Skoryk
NanoMedTech LLC, Kyiv, Ukraine
e-mail: skoryk@nanomedtech.com.ua

polymers that can be produced by anodic alumina nanopatterns. Among them aluminum nanomesh thin films (nano-sized networks non-anodized Al on a substrate) made by electrochemical anodizing and wet etching of porous anodic alumina have special importance as one of the promising candidates for transparent conductive layers (TCLs) which possess both high conductivity and high optical transparency [6–10].

Transparent conductive layers (TCLs) which possess both high conductivity and high optical transparency have many actual and potential applications. Areas of application are optoelectronics, plasmonics, biosensorics, and sources of "green energy." Transparent conducting electrodes are used in light-emitting and solar cells, different kinds of displays, touch screens, etc. [11–15]. Traditionally, films of conductive oxides are used. These are mainly indium tin oxide (ITO) as well as zinc and tin oxides, including doped ones [12, 13]. TCLs on conducting polymers have been also developed [15]. Alternative materials with new operational properties, structure, and morphology are also being searched [14–21]. Nanostructured metal-based thin films as metallic nanowires, metallic and hybrid nanogratings, and metal nanotrough networks are among these materials [19–22].

Aluminum nanomesh thin films made by electrochemical anodizing and wet etching of porous anodic alumina (PAA) are promising candidates for manufacturing of TCL [6–10]. Such Al nanomeshes are electrically conductive, optically transparent, and flexible. The size of the PAA cells and, accordingly, the cells of Al nanomesh can be varied in the range of 10 nm to 1000 nm by varying the electrolyte composition and the anodization regime. The uniform pores arrangement allows improvement of the optical and electrical performance up to ITO layers. The study has shown that the transparency of Al nanomesh on glass can be 10–90% and the conductivity 10–1000 Ω sq^{-1} for 400–800 nm wavelength [6, 10]. Such Al nanomesh can be used in next-generation optoelectronic devices—such as thin-film solar cells, touch screens, and flexible displays [6, 7]. In liquid crystal displays, a nanoset aluminum film can simultaneously be used as a TCL and an orienting surface for nematic crystals [8, 9].

To be widely applicable, the production of nanostructures should be inexpensive and compatible with industrial thin-film technology for manufacturing of optoelectronic devices. These requirements are met by a simple and cheap technology for the production of Al nanomesh from aluminum films deposited on glass, Si, and other substrates.

The possibility of forming Al nanomesh by anodic oxidation is closely related to the structural features of PAA. The nanostructured PAA (Fig. 3.1a) is ideally described as a honeycomb structure that consists of hexagonal cells of a D diameter. The relationship between cell size and anodization voltage can be expressed as a linear dependence $D = \lambda_D \cdot U$, where the coefficient λ_D is approximately 2.5 nm•V^{-1}. In the center of each cell is a pore of $d_p = \lambda_d \cdot U$, λ_d diameter, which equals approximately to 1.3 nm•V^{-1} [23, 24]. The bottom of the pore is separated from the aluminum base by a hemispherical layer of barrier oxide with a thickness h_b. The barrier layer thickness was found to be proportional to the anodizing voltage with a ratio of ~1.2 nm •V^{-1} [23, 24]. In practice, the geometric parameters of
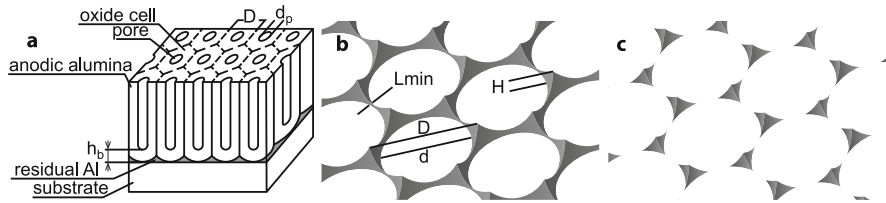
Fig. 3.1 Schematic representation of porous anodic alumina and nanostructures from residual aluminum on a substrate. (**a**) porous anodic alumina; (**b**) Al nanomesh; (**c**) Al nanoprism system

the PAA depend on the anodizing regime (the composition and temperature of the electrolyte, the current or voltage of the anodizing, the duration of anodizing) and aluminum purity [24–26].

The thickness of the walls and the bottom of the pores of the PAA can be reduced by chemical etching, forming the desired pore configuration, for example, for the further production of nanostructures by deposition into pores [27, 28]. It is possible to remove PAA completely and to form a nanostructured surface of aluminum with the purpose of, for example, carrying out the second stage of anodic oxidation [29]. The nanostructured aluminum surface at the oxide/metal interface is a set of concave hemispheres, i.e., has a relief surface with protuberances in the places where the PAA cells meet (Fig. 3.1a). If the formation of PAA is carried out from an aluminum film, then as the bottom surface of the PAA hemispheres reaches the substrate, a continuous aluminum film under the oxide is transformed into a porous aluminum mesh film [6–10]. Al nanomesh on the substrate can be formed by selective etching of the porous oxide (Fig. 3.1b) [6–10].

The size of the cells of Al nanomesh D is equal to the size of the PAA cells. The maximum height H of the aluminum is half the diameter of the PAA pore. The pore diameter d in Al mesh depends both on the anodization voltage and on its duration. The height and thickness of the aluminum mesh decrease as the diameter of the contact surface between the bottom of the PAA pore and the substrate increases during anodic oxidation [16]. By increasing the oxidation time, it is possible to form a nanostructure from individual aluminum nanopyramids (Fig. 3.1c), realized as aluminum hexagonal dot array [30]. Using the dependence of the geometrical parameters on the characteristics of the anodizing process, it is possible to control the morphology of the Al nanostructure and its electrical and optical characteristics [6–10].

The formation of conductive transparent Al nanomesh thin films on substrates includes the following processes (Fig. 3.2):

(a) Vacuum deposition of an aluminum film onto a substrate
(b) Anodic oxidation of the aluminum film to form a PAA (single-stage or two-stage) with stopping when the protruding parts of the anodization front reach the substrate
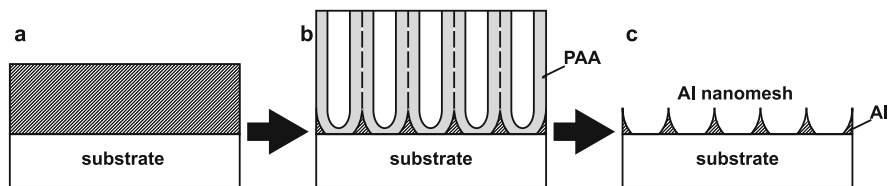(c) Elimination of PAA by selective chemical etching

Fig. 3.2 Schematic depictions show the stages of preparing Al nanomesh thin films on the substrate. (**a**) deposited Al films on substrate; (**b**) PAA and Al nanomesh after anodic oxidation; (**c**) Al nanomesh after elimination of PAA by wet etching

The formation of an ordered Al nanomesh is a way of improving optic-electronic properties by minimizing the number of breakages in aluminum lines and the number of disconnected islands [10]. The homogeneity and ordering of Al nanomesh are determined primarily by the structure of the PAA.

The formation of PAA from deposited Al films differs from the formation of PAA on a massive metal (plate or foil). The structural difference between PAA films grown on massive aluminum and on deposited Al films is connected with differences in the structure of the anodized materials.

To form homogeneous ordered PAA on massive aluminum, annealed and electrochemically polished samples of high-purity aluminum, which have a structure of densely packed large grains and a smooth surface, are usually used. To obtain PAA with homogeneous ordered pores from a bulk aluminum, processes such as annealing of the initial material, electrochemical surface polishing, long anodizing time, and a two-stage anodic oxidation [24–30] are used. As a result of the application of these techniques on massive aluminum, PAA with pores of the same size and having an almost perfect hexagonal ordered structure were obtained.

The use of methods for ordering PAA on massive aluminum is often impossible to apply for deposited aluminum films because of their small thickness and structural features. Vacuum-deposited aluminum films have a granular structure with a considerable difference in sizes of grains and a large number of chaotically located grain boundaries. Their surface may have a high roughness. The density of the aluminum film, the grain size, the degree of randomness of the grain boundaries, and the surface roughness depend on the method and mode of deposition [4, 31–33].

Because of promising perspectives for ordered PAA on substrates to be used for the formation of various nanostructures, a lot of studies has been devoted to this issue [34–38]. The influence of the aluminum film structure on the growth of PAA is being studied. In order to increase the ordering of PAA on aluminum films, two-stage anodizing is sometimes being tried [35, 36, 42], but stable success has not been obtained in this direction so far. Preliminary texturing of the surface by ion beam etching through an electron beam lithography fabricated mask [40] or by transferring patterns from the hard master stamp onto the surface [2, 41] is being successfully applied.

An important point in the formation of PAA and especially Al nanomesh from deposited aluminum films is good adhesion to the substrate. It is necessary to prevent

Al peeling from the substrate during anodizing and etching. The transition metals, active to oxygen, usually Cr, Ta, or Ti [43], are used as an adhesive layer. The Nb layer can also serve as an excellent adhesive layer for thin aluminum films [5]. A careful study of thin Al/Nb films deposited by a magnetron showed that a continuous layer of aluminum is formed even at a 3 nm thickness due to the high affinity of aluminum to niobium [44].

Important issues in the production of Al nanomesh thin films are the control of the stopping time of the anodizing during the formation of Al nanomesh on a substrate and the control of the complete etching of the PAA. Therefore, it is desirable to find an in situ control method, at least for testing the technology. When Al nanomesh formed from Al film, the thickness of the PAA before etching is, as a rule, several hundred nanometers. The effective thickness of the remaining aluminum film lies in the nanometer range. Such thin-film structures of PAA-Al exhibit plasmon and/or waveguide properties. Similar structures served as the basis for the development of optical sensors on metal-clad waveguide (MCWG) with a porous sensor layer [45–48]. The method of optical control directly in the process of formation of the structures of PAA-Al, which comprises monitoring of the angular dependence of reflection on monochromatic light, was used by us earlier for MCWG PAA-Al production. It was used both for the formation of the PAA-Al structures by anodic oxidation and for the widening of pores by wet etching [47]. Since the angular dependencies of the reflection curves of the PAA-Al structures vary both with a change in the dielectric layer and with the slightest change in the thickness of Al, the method can be applied to control the etching of the PAA, as well as to control the remaining Al nanomesh.

This work is devoted to the development and investigation of in situ controlled process for the formation of Al nanomesh from thin aluminum films deposited by a direct current magnetron on glass substrates with an adhesive layer of Nb. In order to control in situ anodic oxidation processes during the formation of the PAA-Al nanomesh structure and the removal of PAA by etching, the method of monitoring of an angular reflection curves was applied. The obtained Al nanomesh was studied by the SEM method. Particular attention is paid to the connection between the features of the initial thin-film structures and the formed Al nanomesh.

3.2 Experiment

The plates of optical polished glass with $n_D = 1.609$, 20×25 mm in size, and 1 mm thick were used as substrates. The substrates were previously cleaned in chromic acid solution for 6 hours. After washing in deionized water, they were treated in the high-frequency oxygen plasma. Immediately prior to the deposition, the final cleaning of the substrate was carried out in the vacuum chamber by bombarding their surface with argon ions with an energy of 400 eV for 10 minutes. Adhesive layer of niobium with a thickness of 2–5 nm and aluminum films with a thickness of 340 nm were deposited in a vacuum chamber equipped with a turbomolecular

pump by magnetron sputtering at a constant current. Optimization of the deposition regime of aluminum films was carried out by us earlier [5]. The parameters related to the deposition of aluminum films are:

Target	Aluminum (99.999% purity)
Gas	Argon (99.95% purity)
Base pressure	$1 \cdot 10 - 6$ Torr
Argon pressure	$1.8 \cdot 10 - 3$ Torr
Substrate-to-target distance	45 mm
Deposition rate	1.1 nm/s

Anodic oxidation of aluminum films was carried out in a two-electrode cell. Anodization modes and control of chronometric dependencies were provided by means of a self-made computerized device. A vacuum-deposited gold film on a glass substrate served as the cathode. The formation of PAA was carried out in the potentiostatic regime, but in the beginning the oxide was grown in a constant current regime. The area for the formation of PAA (100 mm^2) was limited by a mask of photoresist. To avoid etching the aluminum surface in a photoresist developer, the mask was stamped. A 0.3 M solution of oxalic acid was used as the electrolyte. The electrolyte was stirred with a magnetic stirrer, and its temperature was 17 °C. The anodic oxidation was stopped when a sharp jump down appeared on the $I(t)$ curve. Angular reflection curves at a wavelength of 670 nm were monitored using the "Plazmontest" sensor device developed by us [47].

Then selective etching of PAA in an etchant composition of 10% H_3PO_4 + 2% CrO_3 at a temperature of 18 °C was carried out. The change in the reflection curves during etching of PAA was monitored with a self-made instrument providing a large range of light angles incidence.

Samples of aluminum films, PAA, and Al nanomesh have been studied by SEM Tescan Mira 3 LMU. Before the SEM investigations, the Au layer thickness of 8–10 nm was thermally evaporated in vacuum on the surface of the specimens to form a conducting film to avoid the charging problem.

3.3 Results and Discussion

The chronometric dependencies obtained during single-stage anodic oxidation of aluminum films with a thickness of 340 nm at a voltage of 40 V are shown in Fig. 3.3a, b. It is seen from Fig. 3.3b that the stationarity of PAA growth on an aluminum film of 340 nm thickness in this anodization regime is not achieved. We should note that on the curve $I(t)$ (Fig. 3.3b), when the anodization front approaches the substrate, there is always a smooth current drop (Sect. 3.1 on the insert), then a sharp current jump down (Sect. 3.2), and a further gradual decrease (Sect. 3.3). We believe that this jump is due to the fact that the anodization front has reached an
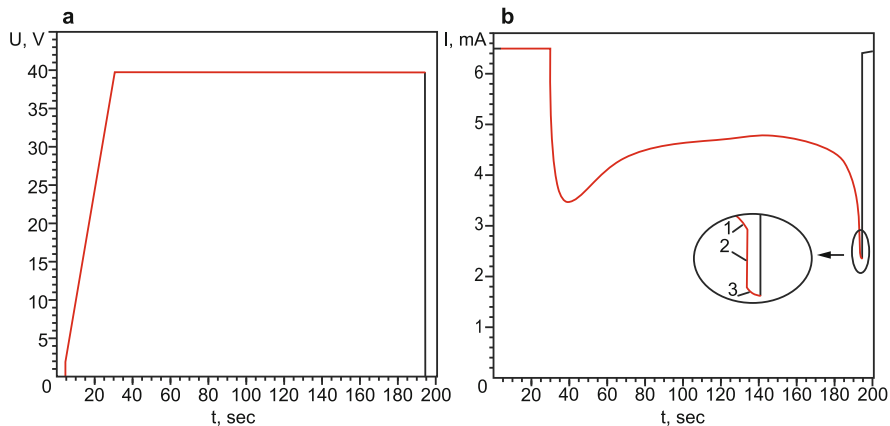
Fig. 3.3 Chronometric dependencies obtained during anodic oxidation of the Al (340 nm)/Nb (adhesive layer) thin-film structure on glass substrate. (**a**) voltage-time characteristic; (**b**) current-time characteristic

adhesive layer. This adhesive layer is probably a mixture of niobium and aluminum atoms due to metal interdiffusion, and it also may be partially oxidized prior to the deposition of aluminum because of the getter properties of niobium. The jump on the curve $I(t)$ we consider as a signal that continuous aluminum has been converted to nanoscale. Further, in the centers of the Al nanomesh cells, nanotips from a mixture of niobium and aluminum oxides are formed, and thinning of the Al lines continues. We stopped the anodizing, as soon as Sect. 3.2 appeared on curve $I(t)$. The decrease in current as the anodization front approaches the substrate occurs very rapidly, and it is difficult to control the time of anodization stoppage reproducibly. To ensure the steady-state growth of the PAA and to ensure the reproducibility of the stopping time, it seems that the anodizing temperature must be lowered.

The minimum angle on the reflection curve of the produced waveguide thin-film structures of PAA/Al was about 64 degrees (in water).

After thorough washing and drying of the samples, we carried out controlled etching of PAA. The control of PAA etching was made by a self-made computerized device with a light source of 670 nm wavelength, *p*-polarizer, and a photodiode. The range of light incidence angles of 40–68 degrees was provided by a stepping motor.

Figure 3.4a shows the scheme for measuring the reflection curves obtained by etching of PAA/Al nanomesh structures. The time interval between the reflection curves was 20 minutes (Fig. 3.4b). The initial curve 1 in Fig. 3.4b is a first-order waveguide mode of a thin-film structure of PAA/Al. In the etching process, the porous oxide layer is gradually etched and converted to a combination of a thin alumina barrier layer and/or PAA residues lying on the surface of the Al nanomesh. The waveguide minimum shifts to the left (curves 2, 3, 4) and gradually disappears, and in the viewing angle region, the left part of the SPR minimum appears (curve 5). When etching proceeds, curve 6 is formed from curve 5. Curve 6 corresponds to
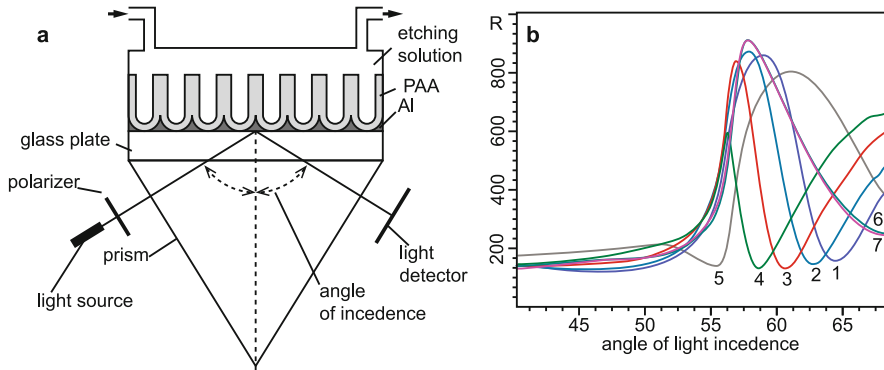
Fig. 3.4 Measurement of the reflection curves during the process of the etching of PAA-Al structure. (**a**) scheme of measurement; (**b**) the reflection curves obtained during the etching of PAA-Al structure

surface plasmon resonance on a nanoscale aluminum film. Due to the limited range of the device angles, we see only the left side of the SPR curve. The invariance of the SPR curve with further etching (curve 7 coincides with curve 6) indicates that PAA is completely etched away. There remained only Al nanomesh, which remained unchanged under this etching regime.

The measured sheet resistance values of such Al nanomesh samples were from 30 Ω/sq. to 45 Ω/sq.

The SEM images shown in Fig. 3.5a, b correspond to the reflection curves 1 and 8 in Fig. 3.4b, respectively. Figure 3.5a is the SEM of the PAA surface after the anodic oxidation. The inset in Fig. 3.5a shows the SEM surface of the original aluminum, which, according to [5], consists of a base aluminum film with protruding crystallites. On the surface of the PAA (Fig. 3.5a), small disordered pores partially covered with gold are seen both on the base surface and on the protruding crystallites. An image of the surface of the sample from which the PAA is etched away shows a surface of Al nanomesh (Fig. 3.5b). Most of the cells have a hexagonal shape, but there are also cells with 5 and 4 vertices. Size of the cells ranges from 90 nm to 120 nm. The nanostructure is heterogeneous, and the discontinuities of Al lines are visible in some places. The width of the aluminum lines is generally about 20 nm. A bright spot measuring 20–25 nm is at the center of almost every cell, apparently a gold-coated bump from an anodic niobium oxide (or a mixture of niobium and aluminum oxides).

SEM of various sections of Al nanomeshes produced from Al films on an adhesive sublayer of Nb are also shown in Fig. 3.6. Figure 3.6a, b correspond to homogeneous and inhomogeneous regions of the nanoscale of aluminum obtained from a film with a thickness of 340 nm. Figure 3.6c is an area of the nanoscale of aluminum obtained from an Al film with a thickness of 1000 nm with protruding crystallites.
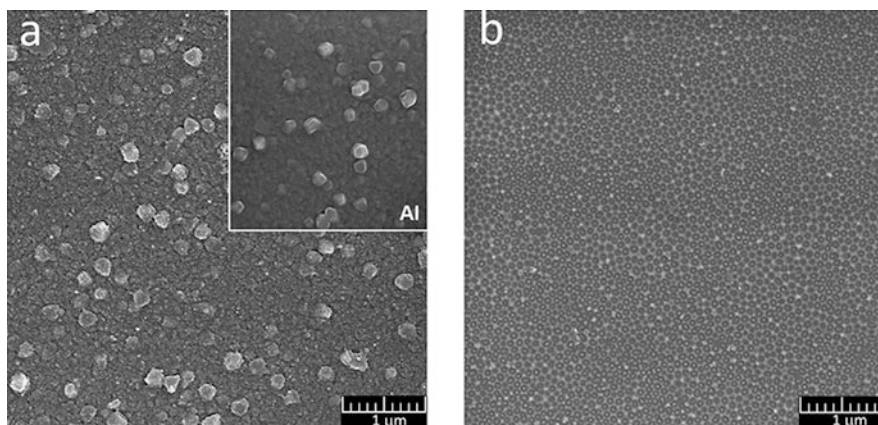
Fig. 3.5 SEM of the PAA and Al nanomesh surface. (**a**) PAA surface after anodic oxidation; (**b**) surface of Al nanomesh after etching of the PAA. The inset in (**a**) shows the surface of the initial aluminum film
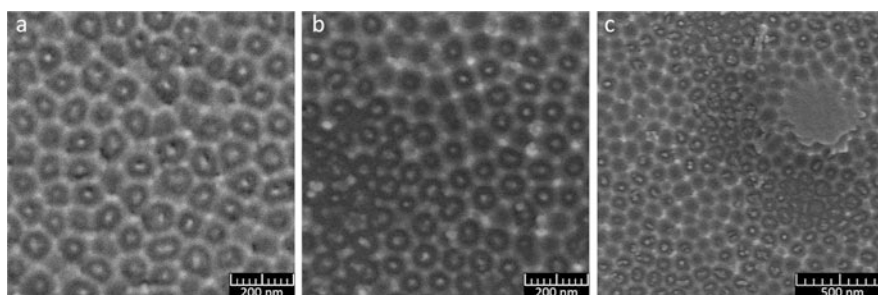

Fig. 3.6 Different sections of Al nanomesh produced from Al films on an adhesive sublayer of Nb. (**a**, **b**) Al nanoscale obtained from Al film with a thickness of 340 nm; (**c**) an area of Al nanoscale obtained from Al film with a thickness of 1000 nm

From the SEM data, we can see that the Al nanomesh reflects to a certain extent the structure of the aluminum film from which it was formed. Places with wider Al lines correspond to places of aluminum film of greater thickness. They are surrounded by the parts of the nanoscale with narrower lines, up to the line ruptures. It seems to us that there are so many reasons that can cause heterogeneity of the Al nanomesh.

First, an Al nanomesh with a nanometer thickness and a width of lines "reacts" to heterogeneity of the thickness of initial Al film. As it was shown earlier [5], the aluminum film (insert in Fig. 3.5a) contains above the "base" the aluminum film, protruding crystallites, and grooves at the grain boundaries. AFM analysis of the relief showed that the roughness of surface (RMS) is 3 nm, difference of the film thickness on areas between protruding crystallites is 10–15 nm, and height of big crystallites is 50–150 nm. The difference in the thickness of the Al film

leads to the fact that different sections of the anodization front reach the substrate not simultaneously. In places where the thickness of aluminum is less, the lower boundary of the barrier layer of PAA reaches the substrate earlier than in places with a greater thickness of aluminum. At these thinner places, formation of nanoscale from aluminum begins earlier. The height and thickness of the Al mesh decrease with the increase in the diameter of the bottom of the pore of the PAA and the substrate, i.e., they decrease with increasing the time of mesh formation [9]. The longer formation time of the nanoscale after touching the bottom of the pore of the cover leads to a thinning of the aluminum lines in places with a lower thickness of the aluminum film. In these places the breaks in the aluminum lines may appear until the anodization stops. As our studies have shown, an increase in the thickness of the initial aluminum film leads to an increase in the inhomogeneity of its thickness [5] and to an increase in the inhomogeneity of the Al nanostructure remaining after the formation of PAA. SEM of the area of Al nanomesh obtained from a film with a thickness of 1000 nm (Fig. 3.6c) clearly shows that the nanoscale formation on the big grain has not yet occurred, whereas around the Al grain, nanomesh already has breaks.

Second, it is likely that the local increase in temperature caused by the current flow in places where the Al nanoset is thinner can further accelerate the oxidation.

Third, the question of the relationship between the purity of aluminum into grains and on grain boundaries remains open, and the purity affects the formation of PAA and, consequently, Al nanoset.

Figure 3.7 shows a schematic representation of the cross section of the samples at different stages of production of Al nanomesh from an Al film on a thin Nb layer corresponding to the SEM images in Figs. 3.5 and 3.6. When drawing up the scheme, we relied on the results of studies on the formation of arrays of nanotips on thin-film Al-Nb structures [49–51]. They show that under the bottom of the pore of the PAA, oxidation of the underlying niobium without its contact with the electrolyte occurs due to the transfer of niobium ions and oxygen by an electric field through a layer of barrier alumina. The migration of O^{2-} and Nb^{5+} ions occurs in each pore along the narrow channel perpendicular to the surface of the substrate. Under the barrier alumina, niobium oxide (or a mixture of niobium and aluminum oxides) is formed, and the aluminum oxide is gradually dissolved. Since niobium oxide has less ion current resistance than alumina, the oxidation of niobium occurs faster than of the neighboring aluminum [49]. Thus, even a very thin adhesive sublayer
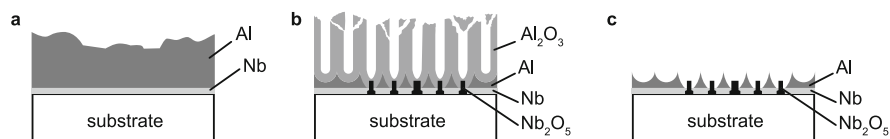

Fig. 3.7 Schematic representation of the cross section of the samples at different stages of fabrication of Al nanomesh from the Al film on the Nb sublayer. (**a**) Al film on Nb adhesive layer; (**b**) appearing of Nb oxide nanotips at the end of anodic oxidation; (**c**) Al nanomesh with Nb oxide nanotips after etching of PAA

of niobium can help preserve the nanoscale from aluminum until the oxidation of niobium under the bottom of the pore is complete.

3.4 Conclusions

An in situ controlled process for the formation of porous anodic alumina and Al nanomesh from thin aluminum films deposited by a direct current magnetron on glass substrates with an adhesive layer of niobium was developed. It was shown that the method of monitoring of the angular reflection curves can be successfully applied in situ not only for monitoring of the anodic oxidation and pore-widening processes in the formation of the structure of PAA-Al [47] but also for monitoring the etching of PAA in Al nanomesh formation.

SEM images of the obtained Al nano-networks show that most cells have a hexagonal shape. A bump from an anodic niobium oxide (or mixtures of niobium and aluminum oxides) is located in the center of almost every cell. We believe that, since the anodic oxidation of Nb occurs faster than that of the neighboring Al, the thin Nb sublayer not only increases the adhesion of aluminum to the substrate but can contribute to the preservation of Al nanomesh when it is formed by anodic oxidation of the aluminum film on the substrate.

Studies by SEM showed that the heterogeneity of the formed Al nanomesh is connected with the structural features of thin aluminum films containing protruding crystallites and cavities at the grain boundaries that disrupt the uniformity of the anodization front during the formation of PAA and Al nanomesh.

The homogeneity of anodic porous alumina and Al nanomesh, in our opinion, can be improved by increasing the uniformity of the thickness of Al films, possibly by precision electrochemical polishing and by using nanopatterning of the aluminum surface prior to anodizing. For the reproducibility of the moment when the formation of the Al nanomesh stops, work should be carried out to optimize the composition of the electrolyte and to decrease the anodic oxidation temperature.

References

1. Losic D, Santos A (2015) Nanoporous alumina: fabrication, structure, properties and applications, Springer Series in Materials Science, vol 219. Springer, Cham
2. Choi J, Nielsch K, Reiche M, Wehrspohn RB, Gosele U (2003) Fabrication of monodomain alumina pore arrays with an interpore distance smaller than the lattice constant of the imprint stamp. J Vac Sci Technol B 21:763–766
3. Ottone C, Laurenti M, Bejtka K, Cauda V (2014) Effects of the film thickness and roughness in the anodization process of very thin aluminum films. J Mater Sci Nanotech 1(1):1–9
4. Lita A, Sanchez JE (1999) Characterization of surface structure in sputtered Al films: correlation to microstructure evolution. J Appl Phys 85(2):876–882

5. Lebyedyeva T, Kryvy S, Lytvyn P, Skoryk M, Shpylovyy P (2016) Formation of nanoporous anodic alumina by anodization of aluminum films on glass substrates. Nanoscale Res Lett 11:203
6. Li Y, Chen Qiu M, Yu H, Zhang X, Sun XW, Chen R (2016) Preparation of aluminum nanomesh thin films from an anodic aluminum oxide template as transparent conductive electrodes. Sci Rep. https://doi.org/10.1038/srep20114
7. Kazarkin B, Mohammed AS, Stsiapanau A, Zhuk S, Satskevich Y, Smirnov A (2014) Transparent conductor based on aluminum nanomesh. J Phys Conf Series. https://doi.org/10.1088/1742-6596/541/1/012027
8. Smirnov A, Stsiapanau A, Mohammed A, Mukha E, Kwok HS, Murauski A (2011) Combined nanostructured layers for display applications. Proceedings SID symposium display week-2011 Los-Angeles, USA, pp 1385–1387
9. Dadivanyan AK, Belyaev VV, Chausov DN, Stepanov AA, Smirnov AG, Tsybin AG, Osipov MA (2015) Nanomesh aluminum films for LC alignment. Theoretical and experimental modeling. Mol Cryst Liq Cryst 611(1):117–122
10. Hubarevich A, Marus M, Stsiapanau A, Smirnov A, Zhao J, Fan W, Wang H, Sun X (2015) Transparent conductive nanoporous aluminium mesh prepared by electrochemical anodizing. Phys Status Solidi A Appl Mater Sci 212(10):2174–2178
11. Gao J, Kempa K, Giersig M, Akinoglu EM, Han B, Li R (2016) Physics of transparent conductors. Adv Phys 65(6):553–617
12. Stadler A (2012) Transparent conducting oxides – an up-to-date overview. Materials 5:661–683
13. Kumar A, Zhou C (2010) The race to replace tin-doped indium oxide: which material will win? ACS Nano 4:11–14
14. Ellmer K (2012) Past achievements and future challenges in the development of optically transparent electrodes. Nat Photon 6:809–817
15. Song TB, Li N (2014) Emerging transparent conducting electrodes for organic light emitting diodes. Electronics 3(1):190–204
16. Zhou Y, Azumi R (2016) Carbon nanotube based transparent conductive films: progress, challenges, and perspectives. Sci Technol Adv Mater 17(1):493–516
17. Park S, Vosguerichian M, Bao Z (2013) A review of fabrication and applications of carbon nanotube film-based flexible electronics. Nanoscale 5(5):1727–1752
18. Rana K, Singh J, Ahn JH (2014) A graphene-based transparent electrode for use in flexible optoelectronic devices. J Mater Chem C 4(2):2646–2656
19. Sannicolo T, Lagrange M, Cabos A, Celle C, Simonato JP, Bellet D (2016) Metallic nanowire-based transparent electrodes for next generation flexible devices: a review. Small 12(44):6052–6075
20. Guo C, Ren Z (2015) Flexible transparent conductors based on metal nanowire networks. Mater Today 18(3):143–154
21. Luo M, Liu Y, Huang W, Qiao W, Zhou Y, Ye Y, Chen LS (2017) Towards flexible transparent electrodes based on carbon and metallic materials. Micromachines 8(12):1–16
22. Wu H, Kong D, Ruan Z, Hsu PC, Wang S, Yu Z, Carney TJ, Hu L, Fan S, Cui Y (2013) A transparent electrode based on a metal nanotrough network. Nat Nanotechnol 8(6):421–425
23. Nielsch K, Choi J, Schwirn K, Wehrspohn RB, Gosele U (2002) Self-ordering regimes of porous alumina: the 10% porosity rule. Nano Lett 2:677–680
24. Sulka G (2008) Highly ordered anodic porous alumina formed by self-organized anodizing, Chapter 1. In: Eftekhari A (ed) Nanostructured materials in electrochemistry. Wiley-VCH, Weinheim
25. Zhang J, Kielbasa JE, Carroll DL (2010) Controllable fabrication of porous alumina templates for nanostructures synthesis. Mater Chem Phys 122:295–300
26. Abd-Elnaiem AM, Gaber A (2013) Parametric study on the anodization of pure aluminum thin film used in fabricating nano-pores template. Int J Electrochem Sci 8:9741–9751

27. Rahman M, Garcia-Caurel E, Santos A, Marsal LF, Pallarès J, Ferré-Borrull J (2012) Effect of the anodization voltage on the pore-widening rate of nanoporous anodic alumina. Nanoscale Res Lett 7(1):474
28. Sulka G, Zaraska L, Stępniowski W (2011) Anodic porous alumina as a template for nanofabrication. In: Nalwa HS (ed) Encyclopedia of nanoscience and nanotechnology, vol 11, 2nd edn. American Scientific Publishers, Stevenson Ranch, pp 261–349
29. Masuda H, Fukuda K (1995) Ordered metal nanohole arrays made by a two-step replication of honeycomb structures of anodic alumina. Sci 268(5216):1466–1468
30. Shingubara S, Murakami Y, Sakaue H, Takahagi T (2001) Formation of Al dot hexagonal array on Si using anodic oxidation and selective etching. Jpn J Appl Phys 41:L340–L343
31. Petrov I, Barna PB, Hultman L, Green JE (2003) Microstructural evolution during film growth. J Vac Sci Technol A 21(5):S117–S128
32. Bordo K, Rubanh HG (2012) Effect of deposition rate on structure and surface morphology of thin evaporated Al films on dielectrics and semiconductors. Mater Sci/Medziagotyra 18(4):313S
33. Her SC, Wang YH (2015) Temperature effect on microstructure and mechanical properties of aluminum film deposited on glass substrates. Indian J Eng Mat Sci 22:268–272
34. Lei Y, Cai W, Wilde G (2007) Highly ordered nanostructures with tunable size, shape and properties: a new way to surface nano-patterning using ultra-thin alumina masks. Prog Mater Sci 52:465–539
35. Chin IK, Yam FK, Chai Y, Hassan Z (2015) Comparative study of porous anodic alumina: effects of aluminium deposition methods. Mater Sci Technol 31(6):709–714
36. Upreti S, Mukherjee K, Palit M, Bag A, Mallik S, Chattopadhyay S, Maiti SK (2014) Porous anodic alumina template formation: deposition technique dependence. In: Physics of semiconductor devices. Springer, Cham, pp 725–728
37. Es-Souni M, Habouti S (2014) Ordered nanomaterial thin films via supported anodized alumina templates. Front Mater 1:1–9
38. Chu SZ, Wada K, Inoue S, Segawa HJ (2011) Direct growth of highly ordered crystalline zirconia nanowire arrays with high aspect ratios on glass by a tailored anodization. Electrochem Soc 158:148
39. Arslan HC, Yusufoglu I, Aslana MM (2014) Structural and optical characterizations of porous anodic alumina–aluminum nanocomposite films on borofloat substrates. Opt Eng 53(7):071822
40. Wang CE, Tanaka S, Saito K, Shimizu T, Shingubara S (2014) Fabrication of ordered arrays of anodic aluminum oxide pores with interpore distance smaller than the pitch of nano-pits formed by ion beam etching. J Mater Sci & Nanotech 1(1):1–6
41. Yasui K, Nishio K, Nunokawa H, Masuda H (2005) Ideally ordered anodic porous alumina with sub-50 nm hole intervals based on imprinting using metal molds. J Vac Sci Technol B 23:L9
42. Chahrour KM, Ahmed NM, Hashim MR, Elfadill NG, Maryam W, Ahmad MA, Bououdina M (2015) Effects of the voltage and time of anodization on modulation of the pore dimensions of AAO films for nanomaterials synthesis. Superlattice Microst 88:489–500
43. Foong TRB, Sellinger A, Hu X (2008) Origin of the bottlenecks in preparing anodized aluminium oxide (AAO) templates on ITO glass. ACS Nano 2(11):2250–2256
44. Imamura T, Hasuo S (1992) Fabrication of high quality Nb/AlOx/-Al/Nb Josephon junctions. II. Deposition of thin Al layers on Nb films. IEEE Trans Appl Supercond 2:84–94
45. Yamaguchi A, Hotta K, Teramae N (2009) Optical waveguide sensor based on a porous anodic alumina/aluminum multilayer film. Anal Chem 81(1):105–111
46. Hotta K, Yamaguchi A, Teramae N (2010) Properties of a metal clad waveguide sensor based on a nanoporous metaloxide/metal multilayer film. Anal Chem 82(14):6066–6073
47. Voitovich ID, Lebyedyeva TS, Rachkov OE, Gorbatiuk OB, Shpylovyy PB (2015) Anodic alumina-based nanoporous coatings for sensory applications. In: Fesenko O, Yatsenko L (eds) Nanoplasmonics, nano-optics, nanocomposites, and surface studies. Springer, Cham, pp 423–431

48. Biednov M, Lebyedyeva T, Shpylovyy P (2015) Gold and aluminum based surface plasmon resonance biosensors: sensitivity enhancement. Proceedings 9506, optical sensors 95061P. https://doi.org/10.1117/12.2177992
49. Surganov V, Gorokh G (2000) Array of niobium nanotips formed in porous anodic alumina matrix. Proc SPIE. https://doi.org/10.1117/12.382321
50. Mozalev A, Sakairi M, Saeki I, Takahashi H (2003) Nucleation and growth of the nanostructured anodic oxides on tantalum and niobium under the porous alumina film. Electrochim Acta 48(20):3155–3170
51. Mozalev A, Vázquez RM, Bittencourt C, Cossement D, Gispert-Guirado F, Llobet E, Habazaki H (2014) Formation–structure–properties of niobium-oxide nanocolumn arrays *via* self-organized anodization of sputter-deposited aluminum-on-niobium layers. J Mater Chem C 2:4847–4860